

Environmental and Chemical Grounds for the Utilization of Blast Furnace Slag in the Production of Binders

E. B. Khobotova and Yu. S. Kalmykova

Kharkiv National Automobile and Highway University, ul. Petrovskogo 25, Kharkiv, 61002 Ukraine
e-mail: loves.1986@mail.ru; chemistry@khadi.kharkov.ua

Received February 22, 2012

Abstract—Mineralogical, elemental, and oxide compositions and morphological surface characteristics of different grain-size fractions of blast furnace slag were determined. The hydraulic activity of blast furnace slag was found to be sufficient for its utilization in the manufacture of binders.

DOI: 10.1134/S1070363212130026

Metallurgical slags, specifically blast furnace slags, approach Portland cement in chemical composition. Problems related to rational disposal of these low-cost materials in the manufacture of binders have long attracted researchers' attention. The building and construction industry utilizes only quenched granulated slag. The use of waste blast furnace slags in the production of binders is strongly limited. Therefore, such waste materials require thorough study to make their utilization in building and construction industry effective and economically profitable.

There are two ways of using blast furnace slag in the production of binders: (1) as a raw material component for the production of Portland cement clinker and (2) joint grinding with cement clinker to obtain Portland blast-furnace cement (PBFC). In the first case, clinkering of slag minerals leads to their decomposition into oxides; therefore, the utility of slags is determined by their oxide composition which should match the oxide composition of raw materials (clay). The weight fractions of oxides, including those occurring as amorphous substances, can be calculated on the basis of elemental composition of a slag. X-Ray powder diffraction method provides determination of oxides in the crystalline part of a slag.

The second way, i.e., utilization of blast furnace slag in the production of PBFC, implies that a slag contains hydraulic minerals. In this case, mineralogical composition of a slag does not change. Hydraulic activity of a slag can be estimated on the basis of its composition and using a set of moduli.

We previously studied the mineralogical, elemental, and oxide compositions of waste blast furnace slags from “Ilyich Iron and Steel Works of Mariupol” Public Corporation [1, 2] and “Dneprovsky Integrated Iron&Steel Works named after Dzershinsky” Public Joint-Stock Company [3], characterized their hydraulic properties, and made recommendations concerning their utilization in the production of binders. Taking into account that slags accumulate natural radioactive elements, their radiation-chemical properties were examined [4], and a procedure for the preparation of radiation-safe PBFC was developed on this basis [5, 6].

The goal of the present work was assess environmental and chemical aspects of utilization of waste blast furnace slag from “Alchevsk Iron & Steel Works” (AISW) Public Joint-Stock Company in the production of binders.

EXPERIMENTAL

The X-ray powder diffraction analysis [7] of blast furnace slag samples from AISW was performed with a Siemens D500 powder diffractometer (copper irradiation, graphite monochromator). Full-profile X-ray powder patterns were obtained in the range $5^\circ < 2\theta < 100^\circ$ with a step of 0.02° ; accumulation time 30 s. Phases were initially identified by searching PDF-1 database [8], and then the patterns were refined by the Rietveld method using FullProf program [9].

The elemental composition of slag was determined by electron probe microanalysis (EPMA) using a JSM-

Table 1. Weight fractions (%) of minerals in different grain-size fractions of AISW blast furnace slag according to the X-ray powder diffraction data

Mineral	<0.63 mm	0.63–1.25 mm	1.25–2.5 mm	2.5–5.0 mm	5.0–10.0 mm	>10 mm
Gehlenite $\text{Ca}_2\text{Al}(\text{Al},\text{Si})_2\text{O}_7$	27.3	32.3	32.1	32.6	34.2	31.8
Pseudowollastonite CaSiO_3^a	16.3	16.6	16.8	14.9	16.4	19.7
Rankinite $\text{Ca}_3\text{Si}_2\text{O}_7$	11.7	13.6	14.1	15.9	16.7	13.8
Bredigite $\text{Ca}_{14}\text{Mg}_2(\text{SiO}_4)_8^a$	15.4	12.2	13.7	12.0	14.1	8.7
Åkermanite $\text{Ca}_2\text{MgSi}_2\text{O}_7^a$	10.3	9.4	8.2	6.9	9.4	14.7
Calcite CaCO_3	7.7	7.0	6.0	6.8	3.0	2.6
Microcline KAlSi_3O_8	3.3	3.9	4.7	4.8	2.9	2.7
Gypsum $\text{CaSO}_4 \cdot 2\text{H}_2\text{O}$	1.8	2.9	2.9	3.5	1.6	3.8
Vesuvianite $\text{Ca}_{19.06}(\text{Al}_{8.82}\text{Mg}_{2.71}\text{Fe}_{1.45}\text{Ti}_{0.16})(\text{SiO}_4)_{10}(\text{Si}_2\text{O}_7)_4\text{O}(\text{OH})(\text{OH})_{6.56}\text{F}_{1.44}$	–	–	–	1.6	0.8	1.1
Quartz SiO_2	6.1	2.3	1.6	1.2	0.9	1.1

^a Hydraulic minerals.

6390 LV scanning electron microscope equipped with an INCA X-ray microanalysis system.

RESULTS AND DISCUSSION

X-Ray powder diffraction (XRPD) analysis of waste blast furnace slag samples from AISW. Incomplete crystallization of slag minerals follows from weak intensities of peaks on all X-ray powder diffraction patterns despite long exposure time. Searching the PDF-1 database matched about 20 phases with appropriate diffraction patterns. Therefore, the results required subsequent Rietveld refinement (Table 1). The major phases in all samples were gehlenite, pseudowollastonite, rankinite, bredigite, and åkermanite; the concentration of other phases was considerably lower. Taking into account that gehlenite and åkermanite are isostructural minerals, they constituted about 40 wt % of each sample.

The concentration of calcite in small-sized fractions was appreciably higher than in large-size fraction; it is formed via reaction of calcium oxide with atmospheric carbon dioxide or via decomposition of complex minerals (vesuvianite) during aging and crystallization of slag. The concentration of gypsum poorly correlated with the elemental analysis data which showed an appreciable amount of sulfur in each fraction. Presumably, the samples contained both anhydrous and hydrated calcium sulfate, among which calcium sulfate

dihydrate is a stable modification detected on the diffractograms.

Transition metals of the 3rd Group detected by elemental analysis did not appear as separate phases on the X-ray powder patterns since they replaced magnesium or aluminum in bredigite, gehlenite, and åkermanite. Sodium was also detected by elemental analysis; it can partly substitute for calcium in calcium-containing phases and isomorphously replace potassium in microcline. Natural microcline usually contains some sodium.

Electron probe microanalysis (EPMA) of blast furnace slag samples from AISW. Table 2 shows the elemental compositions of different slag fractions, determined on the basis of their X-ray spectra. Large-size fractions are characterized by non-uniform composition; therefore, the corresponding percent ranges are given. These data somewhat differ from those derived from the X-ray powder diffraction patterns (Table 1), in particular:

- (1) The EPMA data revealed the presence of sodium, manganese, and titanium in some fractions;
- (2) Chlorine was detected in all grain-size fractions; however, it does not occur in crystalline minerals;
- (3) No fluorine was detected by EPMA, but was detected in vesuvianite by XRPD;
- (4) The weight fraction of sulfur in all samples is higher than that expected from the XRPD data for

Table 2. Elemental composition (wt %) of different grain-size fractions of AISW blast furnace slag according to the electron microprobe analysis data

Element	<0.63 mm	0.63–1.25 mm	1.25–2.5 mm	2.5–5.0 mm	5.0–10.0 mm	>10 mm
Si	11.92	11.49	11.21	9.9–13.58	5.01–6.31	6.32–13.16
Ca	40.0	39.05	38.19	36.57–37.65	38.64–40.91	35.45–56.65
Al	1.96	2.25	1.77	2.35–2.64	0.90–1.32	0.58–2.65
Fe	0.46	0.86	0.68	0.27–0.36	0.30–0.34	0.37–3.17
S	4.30	4.38	5.74	2.41–7.41	9.37–12.57	1.12–2.83
Mg	1.55	1.81	1.50	1.47–2.91	0.66–0.87	1.26–2.06
K	0.265	0.29	0.40	0.56–0.72	0.29–0.38	0.20–0.58
Na	–	0.23	0.26	0.005–0.55	0.15–0.54	0.11–0.38
Mn	0.51	–	0.13	0.044–0.14	0–0.061	0.03–0.07
Ti	0.17	0.25	0.21	0.17–0.22	0–0.11	0.017–0.44
Cl	0.16	0.24	0.21	0.24–0.35	0–0.05	0.16–0.21
O	39.17	39.16	59.33	38.83–40.71	39.80–41.44	33.14–39.05

gypsum; no correlation exists between the concentration of gypsum and sulfur content.

Presumably, compounds of some elements are sorbed by slag minerals, and some slag components may be amorphous substances. This assumption is indirectly supported by the microphotographs of the surface of slag particles (see figure). A highly developed surface area and sorption capacity with respect to particular elements should be noted for the <0.63, 0.63–1.25, and 5.0–10.0-mm fractions. The 5.0–10.0-mm fraction is characterized by needle-shaped surface crystals, and just that fraction was found to contain the largest amounts of chlorine and sulfur, the concentration of gypsum being the lowest.

Amorphous substances were detected on the microphotographs of fractions with a grain size larger than 1.25 mm. The entire surface of slug particles larger than 10 mm was covered by thin short fibers. This fraction displayed increased concentration of Ti and Na.

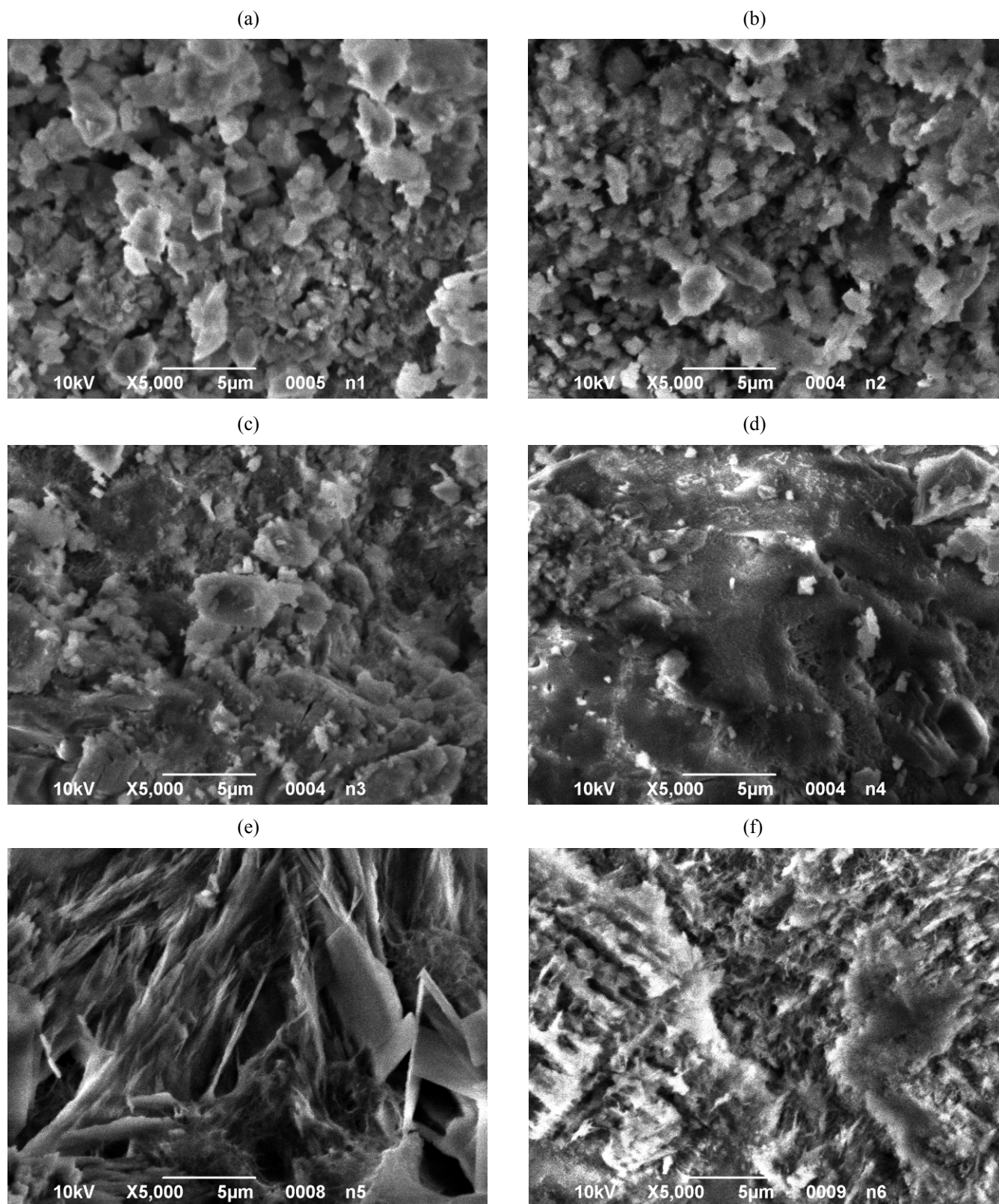
Oxide composition of waste blast furnace slag from AISW. The oxide compositions of different slag fractions were characterized in keeping with their mineralogical compositions given in Table 1 (for the crystalline part) and elemental compositions given in Table 2 (in total). The corresponding data together with module classification are presented in Tables 3 and 4. It may be concluded that some elements are present

only as glassy substances but absent in crystalline minerals. These elements are iron, sulfur, potassium, sodium, manganese, titanium, and chlorine. All other elements constitute both crystalline and amorphous compounds. In all grain-size fractions, the weight concentration of silicon and aluminum oxides in the crystalline phase is higher than in the amorphous phase, while calcium and magnesium oxides show the opposite relation.

The concentration of crystalline aluminum oxide is higher in the 5.0–10.0-mm fraction, whereas its total content is lower. This indicates sharp reduction of the Al_2O_3 content of the amorphous component.

The overall oxide composition of the AISW slag was compared with the data of [10–13] for blast furnace slags from other works in the former USSR. The weight fractions of most oxides in blast furnace slags from different regions were similar. Exceptions were SiO_2 , CaO , and SO_3 whose fractions in the AISW slag were larger. The concentrations of SiO_2 , Al_2O_3 , CaO , and MgO in the crystalline part of the AISW slag fell into the ranges typical of other blast furnace slags; the concentration of MgO was slightly lower, whereas SO_3 , Fe_2O_3 , and alkali metal oxides were absent.

AISW blast furnace slag as a raw material for the production of cement clinker. The overall oxide composition of the AISW blast furnace slag with respect to the major elements does not match the



Scanning electron microscope photographs ($\times 5000$) of the particle surface of AISW blast furnace slag; grain-size fractions, mm: (a) < 0.63 , (b) $0.63-1.25$, (c) $1.25-2.5$, (d) $2.5-5.0$, (e) $5.0-10.0$, and (f) > 10 .

average oxide composition of clays used in the production of Portland cement [11]. However, taking into account approximate specifications of the chemical composition of clay materials for the production of Portland cement [11], the oxide composition of the slag may be regarded as fairly appropriate. According to [11], the concentration of CaO is not limited, the weight fraction of MgO should be no greater than 5%, and of K₂O and Na₂O, no greater than 3–4%, and the concentrations of SiO₂, Al₂O₃, and Fe₂O₃ should fit the required saturation coefficient (SC) and silicate (Ms) and clay moduli (M_{cl}) in the feedstock and clinker. In our case, only SO₃ exceeded the specified weight fraction (1%).

The Ms values for the crystalline phase of almost all grain-size fractions fall into the narrow range of recommended values. The overall oxide compositions give rise to a broad range of Ms values. The clay modulus M_{cl} calculated on the basis of the elemental composition fits the broad range of M_{cl} values specified for raw materials. High saturation coefficients were found for fractions with a grain size of more than 5 mm.

The blast furnace slag from AISW is basic, the basicity modulus Mo being higher than unity. The basicity increases in parallel with the grain size. The crystalline phase is more acidic. According to published data [12], basic blast furnace slags contain 44–48% of CaO, 35–38% of SiO₂, and 5–10% of Al₂O₃. In our case, the concentration of CaO is higher, and the concentrations of SiO₂ and Al₂O₃ are lower.

In keeping with the quality coefficient (QC), all fractions may be regarded as a 1st-grade slag. The quality coefficient increases in going to large-size fractions. The State Standard Specification [14] ranks slags with respect to their chemical composition; in particular the oxide content of a 1st-grade slag should be as follows, %: Al₂O₃, 8.0; MgO, 15.0; TiO₂, 2.0. The AISW blast furnace slag deviates by the alumina content. As noted in [12], active blast furnace slag should contain more than 42% of CaO, 4.5% of SO₃, and less than 1% of MnO. Except for the higher SO₃ content, the other components match the optimal values.

According to the mineralogical classification [10], the blast furnace slag under study belongs to the second most widespread group, i.e., aluminate-free slags (melilite). Sintering of a slag replacing a part of clay component in the feedstock leads to loss of its

hydraulic activity. Sintering yields alumina in a pure form from hydraulically inactive minerals as well, e.g., from gehlenite. Åkermanite decomposes into C₂S and MgO·SiO₂ (or C₂S, CaO, and MgO) [15]. Alkali metal oxides K₂O and Na₂O at a concentration of less than 1% (as in the examined samples) should not exert a negative effect. By contrast, they accelerate transformation of quartz into reactive cristobalite tridymite and improve the solubility of silica. These conditions favor vigorous synthesis of various calcium compounds in slag [15].

Sulfur(VI) oxide may negatively affect sintering of slag-containing feedstock. It is recommended [11] to use slags containing no more than 3.5% of sulfuric anhydride. The observed increased concentration of SO₃ could favor formation of sulfur-containing compounds, the most stable of which being calcium sulfoaluminate 3CaO·Al₂O₃·CaSO₄.

The use of blast furnace slag instead of clay component of cement feedstock may give rise to some specific features in the formation of minerals upon sintering. Crystallization of slag glass generates complex two- and three-component minerals which react with lime at a lower rate than do free oxides. This effect considerably weakens at 1200–1300°C, and it almost disappears at 1450°C [15].

Thus the oxide composition of the AISW blast furnace slag in combination with its moduli give us grounds to recommend it for use in the manufacture of Portland cement clinker as a partial substitute for clay component. In keeping with the saturation coefficients, the use of fractions with a grain size of larger than 5 mm is most advisable.

Waste blast furnace slag from AISW as a component of PBFC. The qualitative oxide composition of the AISW blast furnace slag corresponds to that of PBFC clinker [10, 11]. There are some deviations in quantitative data (except for SiO₂ and Al₂O₃). The concentrations of CaO and Fe₂O₃ are slightly lower, whereas the concentration of SO₃ is higher

Blast furnace slag is characterized by some hydraulic activity, as follows from the major oxide ratios and calculated moduli (Tables 3, 4). The concentration of silica is lower than the overall concentration of CaO and Al₂O₃. In this case, SiO₂ does not inhibit crystallization and hydration of compounds that constitute the slag. Calcium oxide is present only in minerals with different hydraulic activities. No free CaO is present.

Table 3. Weight fractions of oxides (%) in different grain-size fractions of AISW blast furnace slag according to the X-ray powder diffraction data and their classification according to the modulus system

Oxide	<0.63 mm	0.63–1.25 mm	1.25–2.5 mm	2.5–5.0 mm	5.0–10.0 mm	>10 mm
SiO ₂	37.45	34.55	34.64	33.01	34.78	35.26
CaO	45.03	45.84	46.08	45.39	46.91	45.0
Al ₂ O ₃	10.76	12.73	12.80	13.01	13.25	12.32
Fe ₂ O ₃	–	–	–	–	–	–
SO ₃	–	–	–	–	–	–
MgO	1.51	1.38	1.21	1.01	1.38	2.16
Na ₂ O	–	–	–	–	–	–
K ₂ O	–	–	–	–	–	–
MnO	–	–	–	–	–	–
TiO ₂	–	–	–	–	–	–
Cl ₂ O	–	–	–	–	–	–
Modulus						
$Mo = \frac{CaO + MgO}{SiO_2 + Al_2O_3 + Fe_2O_3} \geq 1.0 [10]$	0.97	1.0	1.0	1.01	1.01	0.99
$Ms = \frac{SiO_2}{Al_2O_3 + Fe_2O_3}$ <p>Reference values: raw material, 1.8–3.3 [13], 2.62–7.11 [11]; clays, 1.8–3.75 [11]; PBFC component, 1.7–3.5 [11]</p>	3.48	2.71	2.71	2.54	2.62	2.86
$Ma = \frac{Al_2O_3}{SiO_2}$ <p>Reference values for active mineral dopes: grade I, ≥ 0.25; grade II, ≥ 0.20; grade III, ≥ 0.12 [11]</p>	0.29	0.37	0.37	0.39	0.38	0.35
$M_{hydr} = \frac{CaO}{SiO_2 + Al_2O_3 + Fe_2O_3}$ <p>1.7–2.4 [13]</p>	0.93	0.97	0.97	0.99	0.98	0.95
$M_{cl} = \frac{Al_2O_3}{Fe_2O_3}$ <p>Reference values: raw material, 1.5–2.5 [13], 6.99–28.67 [11]; clays, 1.6–4.1 [11]; PBFC component 1.0–2.5 [11]</p>	–	–	–	–	–	–
$QC = \frac{CaO + MgO + Al_2O_3}{SiO_2 + MnO}$ <p>Reference values: grade I, ≥ 1.65; grade II, ≥ 1.45; grade III, ≥ 1.20 [14]</p>	1.53	1.74	1.73	1.80	1.77	1.69
$SC = \frac{CaO - (1.65Al_2O_3 + 0.35Fe_2O_3)}{2.88SiO_2}$ <p>Reference value for PBFC component 0.85–0.95 [11]</p>	0.26	0.26	0.26	0.26	0.26	0.25

Table 3. (Contd.)

Oxide	<0.63 mm	0.63–1.25 mm	1.25–2.5 mm	2.5–5.0 mm	5.0–10.0 mm	>10 mm
Saturation coefficient according to Lea–Parker $SC = \frac{100CaO}{2.8SiO_2 + 1.18Al_2O_3 + 0.65Fe_2O_3}$ Reference value for raw material 85–100 [13]	38.3	40.7	41.1	42.1	41.5	39.7
Saturation coefficient according to Kind–Jung $SC = \frac{CaO - (1.65Al_2O_3 + 0.35Fe_2O_3 + 0.7SiO_2)}{1.8SiO_2}$ Reference value for raw material 0.92–0.95 [13]	0.01	0.007	0.007	0.009	0.007	–

Table 4. Weight fractions of oxides (%) in different grain-size fractions of AISW blast furnace slag according to the electron microprobe analysis data and their classification according to the modulus system

Oxide	<0.63 mm	0.63–1.25 mm	1.25–2.5 mm	2.5–5.0 mm	5.0–10.0 mm	>10 mm
SiO ₂	25.5	24.59	23.99	21.15–29.05	10.73–13.51	13.51–28.15
CaO	55.97	54.64	53.43	51.17–52.68	54.07–57.24	49.6–79.26
Al ₂ O ₃	3.70	4.24	3.35	4.43–4.98	1.69–2.49	1.1–5.0
Fe ₂ O ₃	0.66	1.23	0.98	0.38–0.52	0.43–0.49	0.52–4.54
SO ₃	10.73	10.93	14.34	6.01–18.5	23.39–31.39	2.8–7.07
MgO	2.57	3.0	2.48	2.44–4.82	1.09–1.44	2.09–3.41
Na ₂ O	–	0.31	0.35	0.01–0.74	0.2–0.73	0.15–0.52
K ₂ O	0.32	0.35	0.48	0.68–0.87	0.34–0.46	0.25–0.7
MnO	0.066	–	0.16	0.06–0.17	≤0–0.079	0.04–0.09
TiO ₂	0.28	0.42	0.07	0.28–0.36	≤0.18	0.03–0.73
Cl ₂ O	0.20	0.30	0.38	0.29–0.43	≤0.06	0.20–0.25
Modulus						
$Mo = \frac{CaO + MgO}{SiO_2 + Al_2O_3 + Fe_2O_3} \geq 1.0$ [10]	1.96	1.92	1.97	1.66–2.07	3.56–4.29	2.19–3.42
$Ms = \frac{SiO_2}{Al_2O_3 + Fe_2O_3}$	5.85	4.5	5.54	4.4–5.28	4.53–5.06	2.95–8.34
Reference values: raw material, 1.8–3.3 [13], 2.62–7.11 [11], clays, 1.8–3.75 [11]; PBFC component, 1.7–3.5 [11]						
$Ma = \frac{Al_2O_3}{SiO_2}$	0.15	0.17	0.14	0.17–0.21	0.16–0.18	0.08–0.18
Reference values for active mineral dopers: grade I, ≥0.25; grade II, ≥0.20; grade III, ≥0.12 [11]						

Table 4. (Contd.)

Oxide	<0.63 mm	0.63–1.25 mm	1.25–2.5 mm	2.5–5.0 mm	5.0–10.0 mm	>10 mm
$M_{\text{hydr}} = \frac{\text{CaO}}{\text{SiO}_2 + \text{Al}_2\text{O}_3 + \text{Fe}_2\text{O}_3}$ 1.7–2.4 [13]	1.87	1.82	1.89	1.52–1.97	3.47–4.21	2.10–3.28
$M_{\text{cl}} = \frac{\text{Al}_2\text{O}_3}{\text{Fe}_2\text{O}_3}$ Reference values: raw material, 1.5–2.5 [13], 6.99–28.67 [11]; clays, 1.6–4.1 [11]; PBFC component, 1.0–2.5 [11]	5.6	3.45	3.42	9.58–11.66	3.93–5.08	1.1–2.12
$QC = \frac{\text{CaO} + \text{MgO} + \text{Al}_2\text{O}_3}{\text{SiO}_2 + \text{MnO}}$ grade I, ≥ 1.65 ; grade II, ≥ 1.45 ; grade III, ≥ 1.20 [14]	2.43	2.52	2.45	2.14–2.74	4.5–5.3	3.1–3.9
$SC = \frac{\text{CaO} - (1.65\text{Al}_2\text{O}_3 + 0.35\text{Fe}_2\text{O}_3)}{2.88\text{SiO}_2}$ Reference values for PBFC component 0.85–0.95 [11]	0.70	0.69	0.71	0.54–0.74	1.4–1.7	0.88–1.26
Saturation coefficient according to Lea–Parker $SC = \frac{\text{CaO} - (1.65\text{Al}_2\text{O}_3 + 0.35\text{Fe}_2\text{O}_3)}{2.88\text{SiO}_2}$ Reference value for raw material 85–100 [13]	73.5	73.2	74.5	60.2–79.1	139.3–167.3	90.4–125.7
Saturation coefficient according to Kind–Jung $SC = \frac{\text{CaO} - (1.65\text{Al}_2\text{O}_3 + 0.35\text{Fe}_2\text{O}_3 + 0.7\text{SiO}_2)}{1.8\text{SiO}_2}$ Reference value for raw material 0.92–0.95 [13]	0.45	0.44	0.46	0.29–0.49	1.15–1.45	0.63–1.01

The chemical composition of a blast furnace slag as a hydraulic component of high early-strength blast-furnace cements of grade 400–500 is expressed most often as $M_o = 0.95$ – 1.2 and $M_s = 1.1$ – 2.0 [16]. However, depending on the properties of ores and fuel, the moduli of blast furnace slag may vary over a broad range, $M_o = 0.65$ – 1.3 and $M_s = 1.2$ – 7.0 [16] or 1.7 – 3.5 [11]. The examined samples are more basic than it is recommended; and their M_s values cover the broadest range.

According to obsolete classification [11], the hydraulic activity modulus corresponds to grade III basic slags as active minerale dopes with an M_a value of ≥ 0.12 . The M_a value for the crystalline part of all grain-size fractions is considerably higher, and it fits grade I slags. The hydraulic moduli M_{hydr} of only fractions smaller than 5 mm fall into the optimal range, and the hydraulic activity of the crystalline phase is lower than the total one. The alumina moduli of all fractions are very high; except for the large-size fraction (>10 mm), they go beyond the upper limit of

the optimal range. The saturation coefficient matches the optimal range only for large-size fractions (>5 mm). The saturation coefficient of the crystalline phase is considerably lower.

The use of blast furnace slag as a component of PBFC is eventually determined by hydraulic activity of its constituent minerals. The AISW blast furnace slag contains minerals belonging to three systems (Table 1). The CaO – SiO_2 system is represented by rankinite ($3\text{CaO} \cdot 2\text{SiO}_2$), bredigite ($\alpha\text{-}2\text{CaO} \cdot \text{SiO}_2$), and pseudowollastonite ($\alpha\text{-CaO} \cdot \text{SiO}_2$). Rankinite (tricalcium disilicate) possesses no hydraulic activity. Unlike rankinite, bredigite and pseudowollastonite undergo hydration and harden.

Gehlenite ($2\text{CaO} \cdot \text{Al}_2\text{O}_3 \cdot \text{SiO}_2$) belongs to the ternary CaO – Al_2O_3 – SiO_2 system. It does not possess binding capacity and impairs the quality of aluminate cement. Åkermanite ($2\text{CaO} \cdot \text{MgO} \cdot 2\text{SiO}_2$; CaO – MgO – SiO_2 ternary system) is an island silicate possessing a weak hydraulic activity.

According to the XRPD data, the weight fraction of hydraulic minerals changes from 33.7% to 43.1% (Table 1), depending on the particle size. The highest concentration of hydraulic minerals was found for the large-size fraction (>10 mm; 43.1%). Therefore, waste blast furnace slag from AISW, especially its fractions with a grain size of 5 mm and more, may be recommended for use in the production of Portland blast-furnace cement.

REFERENCES

1. Khobotova, E.B. and Kalmykova, Yu.S., *Ekol. Promst.*, 2011, no. 1, p. 35.
2. Kalmykova, Yu.S., *Sbornik nauchnykh trudov XVIII Mezhdunarodnoi nauchno-tehnicheskoi konferentsii "Ekologicheskaya i tekhnogennaya bezopasnost". Okhrana vodnogo i vozdušnogo basseinov. Utilizatsiya otkhodov* (Collection of Scientific Papers, XVIIIth Int. Scientific-Technical Conf. "Environmental and Technological Safety. Water and Air Protection. Disposal of Wastes"), Kharkiv: UkrVODGEO, 2010, p. 73.
3. Kalmykova, Yu.S., Khobotova, E.B., Tolmachev, S.N., and Ukhanyova, M.I., *Sbornik trudov XIX Mezhdunarodnoi nauchno-prakticheskoi konferentsii "KAZANTIP-EKO-2011. Innovatsionnye puti resheniya aktual'nykh problem bazovykh otraslei, ekologii, energo- i resursosberezheniya"* (Proc. XIXth Int. Scientific-Practical Conf. "KAZANTIP-EKO-2011. Innovation Methods for the Solution of Urgent Problems in the Basic Industries, Ecology, and Energy and Resource Saving"), Kharkiv: NTMT, 2011, vol. 2, p. 339.
4. Khobotova, E.B., Ukhanyova, M.I., and Kalmykova, Yu.S., *Ekol. Promst.*, 2009, no. 3, p. 49.
5. Ukhanyova, M.I., Khobotova, E.B., and Kalmykova, Yu.S., *Ekol. Promst.*, 2010, no. 2, p. 45.
6. Khobotova, E.B., Ukhanyova, M.I., and Kalmykova, Yu.S., Ukrainian Patent no. 41 223, 2009.
7. Bokii, G.B. and Porai-Koshits, M.A., *Rentgenostrukturnyi analiz* (X-Ray Analysis), Moscow: Mosk. Gos. Univ., 1964, vol. 1.
8. *JCPDS PDF-1 File*. International Committee for Diffraction Data, release 1994, PA, USA.
9. Rodriguez-Carvajal, J. and Roisnel, T., *FullProf.98 and WinPLOTR: New Windows 95/NT Applications for Diffraction*. Commission for Powder Diffraction, International Union of Crystallography, Newsletter no. 20 (May–August), 1998.
10. Perepelitsyn, V.A., *Osnovy tekhnicheskoi mineralogii i petrografii* (Basic Principles of Technical Mineralogy and Petrography), Moscow: Nedra, 1987.
11. *Spravochnik po proizvodstvu tsementa* (Cement Production. Reference Book), Kholin, I.I., Ed., Moscow: Gosstroizdat, 1963.
12. Reznichenko, P.T. and Chekhov, A.P., *Okhrana okruzhayushchei sredy i ispol'zovanie otkhodov promyshlennosti* (Environmental Protection and Industrial Waste Utilization), Dnepropetrovsk: Promin', 1979.
13. Kužvart, M., *Industrial Minerals and Rocks*, Amsterdam: Elsevier, 1984. Translated under the title *Nemetallicheskie poleznye iskopaemye*, Moscow: Mir, 1986.
14. GOST 3476-74 "Shlaki domennye i elektrotermofosfornye granulirovannye dlya proizvodstva tsementov" (State Standard Specification no. 3476-74 "Granulated Blast-Furnace and Electrothermophosphorus Slags for the Production of Cements").
15. Butt, Yu.M., *Portlandtsementnyi klinker* (Portland Cement Clinker), Butt, Yu.M. and Timashev, V.V., Eds., Moscow: Stroiizdat, 1967.
16. Budnikov, P.P. and Znachko-Yavorskii, I.L., *Granulirovannye domennye shlaki i shlakovye tsementy* (Granulated Blast Furnace Slags and Cements), Moscow: Promstroizdat, 1953.